Role of Solute Segregation on Microstructure and Mechanical Properties of Zircaloy-4

M. Ahmad, J.I. Akhter, M.A. Shaikh, M. Iqbal, and W. Ahmad

(Submitted 19 March 2002; in revised form 16 January 2003)

The microstructure of two different lots of Zircaloy-4 was investigated by using a scanning electron microscope (SEM) attached to an energy dispersive system (EDS). The alloy containing Ni higher than the ASTM specification shows parallel plate structure with segregation of Ni, Fe, and Cr at the triple points of β-grains, and it failed during forging due to crack initiation. The second alloy having Ni content within the ASTM specification has basketweave morphology with minute segregation of Fe and Cr and was forged successfully. The absorbed energy is higher for the successfully forged alloy than for the alloy that failed during forging. It was also observed that the fracture started from the segregated area rich in Ni, Fe, and Cr, and propagated along the plate. The alloy with parallel plate structure is harder than the alloy with basketweave structure.

Keywords impact energy, microhardness, microstructure, segregation, Zircaloy-4

1. Introduction

Zircaloy-4 is used as a cladding material for fuel elements in the nuclear industry.[1] In zirconium alloys, the elements like Fe, Cr, and Ni present in solid solution at high temperature, lead to the formation of intermetallic compounds during cooling.[2] These compounds are brittle and have the ability to absorb large amounts of hydrogen. Furthermore, since Ni has higher diffusivity in Zircaloy-4,[3] its presence results in increased hydrogen absorption during corrosion in high temperature water and steam.[4] Hydrogen forms zirconium hydride precipitates in Zircaloy-4 causing hydrogen embrittlement, which reduces fracture toughness and ductility.[5] Therefore, the presence of Ni, even in small amounts, can affect the properties of Zircaloy-4.

Nominally similar batches of Zircaloy may produce two markedly different structures. One is the normal "basketweave" structure typical of zirconium alloys resulting from random precipitation of α-plates on a number of planes in one β-grain. The other is a "parallel plate" Widmanstatten structure in which most of the α-plates in one prior β-grain precipitate on the same habit plane.[6] This difference has been attributed to the presence of randomly dispersed second phase particles, which appear to nucleate α-plates in the alloy producing a "basketweave" structure. The "parallel plate" structure is expected to yield lower ductility because aggregates of equally oriented parallel plates would behave as coarse grain.[7] Moreover, α-plates nucleates at nearly 20 °C less undercooling when the material contains second phase particles, which are insoluble at higher temperature where the transformation is slower. The interference of plates nucleated randomly on a number of habit planes in the β-grain would result in slower kinetics than would be expected from plates growing on parallel planes in the same direction away from the β-boundaries. A particular β-grain boundary may be expected to energetically favor nucleation on a particular plane, and this gives rise to parallel α-plates that would grow to the entire width of the β-grain without interference.

During the preparation of the alloy, compositional segregation may occur because the alloying elements are rejected during solidification at the solid-liquid interface, developing a higher concentration in the remaining liquid. Thus the material last solidified is rich in one or more constituents, and this compositional segregation affects the corrosion properties as well as mechanical properties of the Zircaloy-4.[8] The aim of the current study is to investigate the microstructure of two heats of the alloy: one that failed during forging and the other forged successfully.

2. Experimental

The chemical composition of the two alloys, along with ASTM specification, are given in Table 1. Gas contents of the alloys are listed in Table 2. The samples were polished and etched in a solution of H_2O_2, HNO_3, and HF in 6:6:1 ratio. The etched specimens were examined in a scanning electron microscope (SEM) having an energy dispersive system (EDS) facility.

The Charpy V-notch specimens were prepared to measure the absorbed energy at room temperature. The fractured surfaces were also examined in SEM to investigate the nature of the fracture and to find the cause of crack initiation. Vicker's microhardness measurements were performed using a load of 1.96N.

3. Results and Discussion

SEM examination of the samples, taken from the ingots designated as A and B, revealed a marked difference between the grain structure of the two alloys as shown in Fig.1(a) and

M. Ahmad, J.I. Akhter, M.A. Shaikh, M. Iqbal, and **W. Ahmad,** Nuclear Physics Division, Pakistan Institute of Nuclear Science and Technology, P.O. Nilore, Islamabad, Pakistan. Contact e-mail: jiakhter@yahoo.com.

Table 1 Chemical Composition of Zircaloy-4 Ingots

Specimen Identification	Wt.%				Concentration ppm										
	Sn	Fe	Cr	Zr	Al	B	C	Co	Cu	Hf	Mn	Ni	Si	Ti	W
A	1.57	.197	.088	bal.(a)	21	<5	870	<10	20	60	<20	430	40	<30	<50
B	1.38	.20	.090	bal.	20	<5	480	<10	…	50	<10	<50	<40	…	…
Specification, ASTM	1.2-1.7	.18-.24	.07-.13	bal.	75	5	270	20	50	200	50	70	120	50	100

(a) bal., balance quantity

Table 2 Gaseous Contents in the Zircaloy-4 Ingots

Alloy Designation	Hydrogen, ppm	Oxygen, ppm	Nitrogen, ppm
A	15 ± 1	767 ± 93	55
B	17 ± 8	1408 ± 217	118 ± 15
Specification of ASTM	25	1600	65

(b). Alloy A has generally a parallel plate type structure with the "basketweave" pattern in some localized areas, whereas alloy B has mostly the "basketweave" type structure throughout the material. The size of the plate in alloy B is more uniform than that in alloy A.

Suitable nucleation of second phase particles in Zircaloy-4 depends upon the presence of carbon, oxygen, and nitrogen, as well as phosphorus.[6] These phases are insoluble in β-Zr and are responsible for the nucleation of the "basketweave" structure in the alloy. In the absence or relative scarcity of these solutes, nucleation occurs at the β-grain boundaries and leads to a parallel plate morphology. Oxygen would be expected to have a strong effect on the formation of such phases.[7] Formation of secondary phases enriched in Zr, Fe, and Cr were observed on the grain boundaries in alloy B, whereas Zr-, Fe-, Cr-, and Ni-enriched phases were found in alloy A. There is a regular distribution of Cr and Fe-rich precipitates along the grain boundaries and in the grains in alloy B. The nucleation of a "basketweave" structure of grains in this alloy during cooling may be due to homogeneous distribution of secondary phases or impurity elements. On the other hand, inhomogeneous precipitation was observed in the grain and along the grain boundaries in alloy A.

Another difference between the microstructures of the two alloys is the presence of localized areas of segregated phases. These areas are small and rare in alloy B, whereas large segregated areas are found in alloy A. Most of the segregation areas were observed at triple points and at the grain boundaries in both the alloys. Such areas in A and B are shown in Fig. 2(a) and (b). Chemical composition data of the segregated areas (Table 3) indicate the presence of hard and brittle intermetallics.[9] The segregation of these intermetallics at the grain boundaries can be the major cause of crack initiation. The propagation of cracks is assisted by the presence of parallel plate structure. Hardness of the different grains on the etched specimens of both alloys was measured. The values determined are given in Table 4. The hardness of both the coarse and the fine plates in alloy A is much higher than that in alloy B. This increase in hardness is due to the presence of high Ni and its structural effect in alloy A.

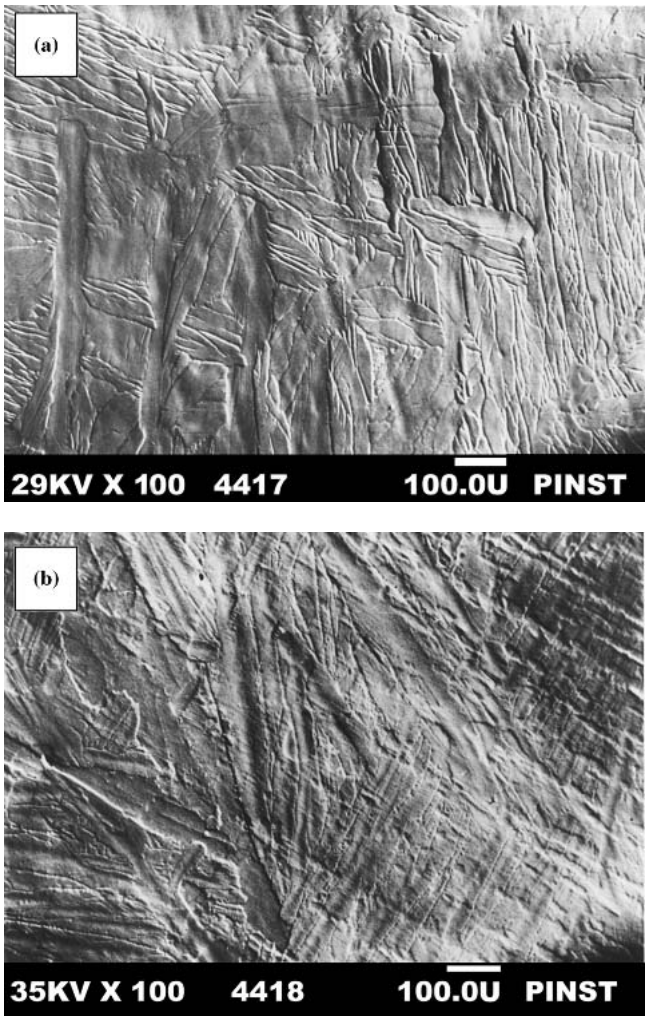

Fig. 1 **(a)** Basketweave type structure in alloy B; **(b)** parallel plate type structure in alloy A

Ökvist and Källström[7] mention that the alloy with higher carbon concentration (100-200 ppm) has "basketweave structure" and that with low carbon concentration (<50 ppm) has parallel plate structure. In our study, alloy A has a higher concentration of carbon than alloy B (870 ppm versus 480 ppm). This means that concentration of carbon is higher than ASTM specifications in both the alloys, and should be sufficient to form the homogeneous distribution of ZrC required for the formation of basketweave structure. However, we observe parallel plate structure in alloy A and basketweave structure in alloy B. In our results, the Ni content in alloy A is found to be

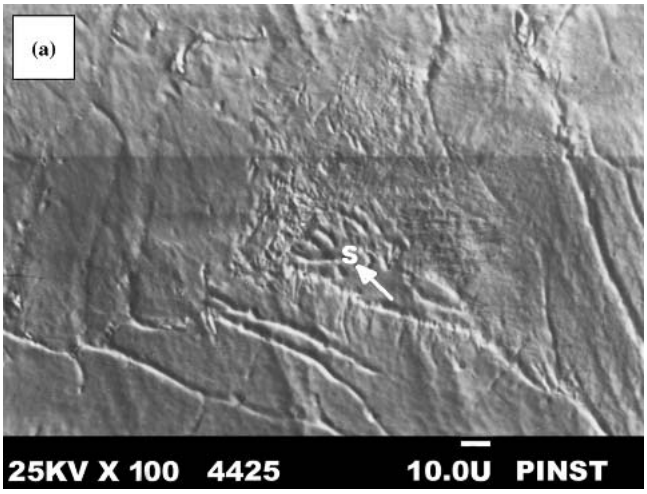

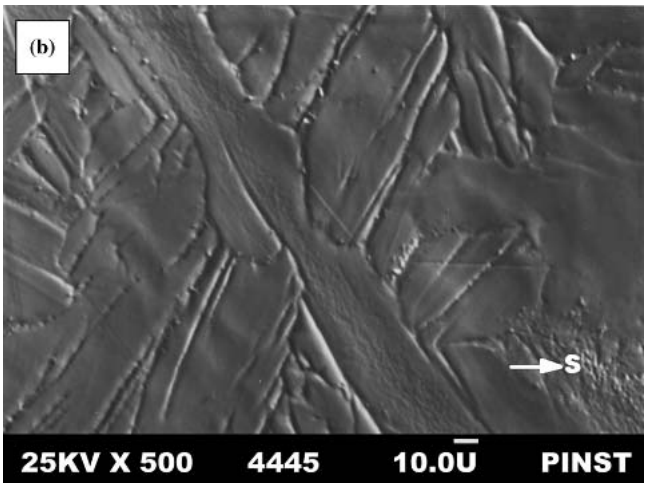

Fig. 2 Segregation areas in **(a)** alloy A; **(b)** alloy B

Table 3 Composition in wt.% of Segregated Areas

Element	Alloy A	Alloy B
Cr	0.3-1.1	0.1-1.1
Fe	1.1-4.5	0.2-3.2
Ni	0.5-3.0	…
Sn	0.4-1.1	0.2-1.8
Zr	93.5-95.1	95.1-98.9

Table 4 Impact Properties and Average Microhardness Values

Specimen Identification	Energy Absorbed, J	Lateral Expansion, mm	Hardness, HV	
			Coarse Plates	Fine Plates
A	4.5	0.02	145	255
B	12.5	0.032	110	175

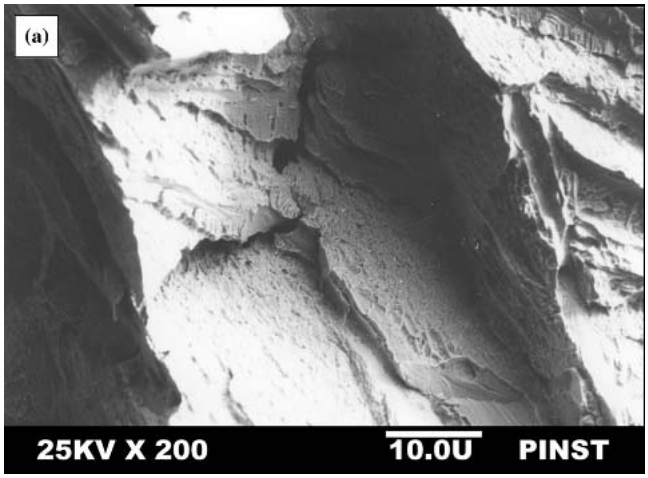

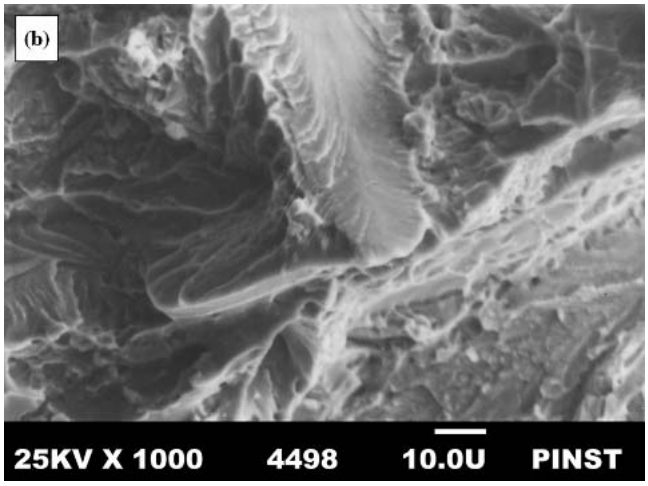

Fig. 3 **(a)** Cleavage fracture along with cracks in alloy A; **(b)** formation of flutes in alloy A

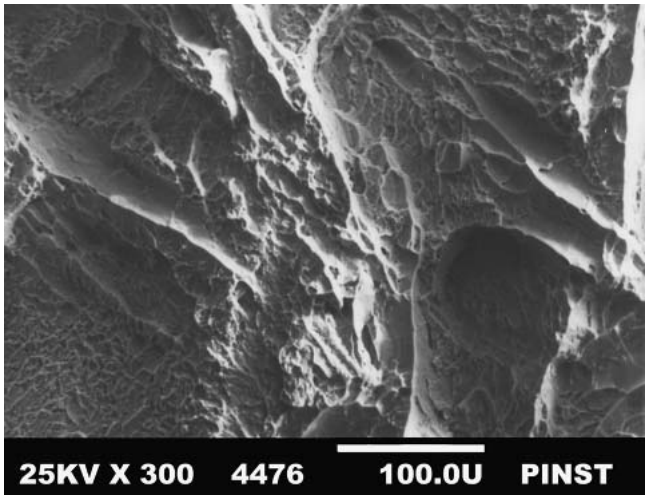

Fig. 4 Ductile fracture in alloy B

430 ppm, which is very high compared with the ASTM specification of 70 ppm. It is observed that Ni segregates at the triple points of β-grains along with Fe and Cr. Segregation of these elements at the triple points hinders the homogeneous distribution of second phase particles responsible for the formation of basketweave structure.

SEM studies of the fractured surfaces revealed the cleavage lines and flutes in alloy A (Fig. 3a,b), while only the dimples were observed in alloy B (Fig. 4). Cleavage fracture is a low energy fracture that propagates along well-defined low-index crystallographic planes, while flutes are ruptured halves of tubular voids, which are formed by the planar intersecting slip mechanism.[10-12] The absorbed energy of alloy A is lower than that of alloy B, which is confirmed by the presence of cleavage lines and flutes. In Fig. 3(a), cracks and cleavage lines were seen. It was also observed that the cracks were initiating from the segregated areas highly enriched in Ni, Fe, and Cr, and these areas are marked as "S". Initiation of the cracks from the segregated area is due to the formation of hard and brittle intermetallic phases at these areas.

4. Conclusion

On the basis of the investigations, the probable reasons for the failure of alloy A during forging are as follows:

- A large and localized area with segregation of Ni, Fe, and Cr is the source of crack initiation.
- The large amount of Ni in alloy A compared with alloy B is the source of large and localized segregated areas.
- The microstructure of alloy A has parallel plate morphology, which assists the crack propagation.
- The inhomogeneous distribution of second phase particles causes the parallel plate structure instead of basketweave structure.

References

1. J.B. Bai, C. Prioul, S. Lansiart, and D. Francois: "Brittle Fracture Induced by Hydrides in Zircaloy-4," *Scr. Metall. Mater.*, 1991, *25*, pp. 2559-63.
2. K. Loucif, R. Borrelly, and P. Merle: "Study by Thermoelectric Power and Resistivity Measurements of the Precipitation Kinetics in Zirconium Alloys Between 450 and 600 °C," *J. Nucl. Mater.*, 1992, *189*, pp. 34-45.
3. H.I. Shaaban, F.H. Hammad, and J.L. Baron: "Diffusion Bonding of Stainless Steel to Zircaloy-4 in the Presence of an Iron Intermediate Layer," *J. Nucl. Mater.*, 1978, *78,* pp. 431-33.
4. W.E. Berry, D.A. Waughan, and E.L. White: "Hydrogen Pickup During Aqueous Corrosion of Zirconium Alloys," *Corrosion*, 1961, *17,* pp. 109t-117t.
5. J.B. Bai, C. Prioul, and D. Francois: "Effect of Microstructure Factors and Cold Work on the Hydride Precipitation in Zircaloy-r Sheet," *J. Adv. Sci.*, 1991, *3*(4), pp. 188-200.
6. R.A. Holt: "The Beta to Alpha Transformation in Zircaloy-4," *J. Nucl. Mater.*, 1970, *35*, pp. 322-34.
7. G. Ökvist and K. Källström: "The Effect of Zirconium Carbide on the $\beta \rightarrow \alpha$ Transformation Structure in Zircaloy," *J. Nucl. Mater.*, 1970, *35*, pp. 316-21.
8. W. Reitz, R. Graham, P. Danielson, and J. Rawers: "Compositional Segregation and Its Effect on Corrosion of Laser-Processed Zircaloy-4," *J. Mater. Sci. Letts.,* 1990, *9*(12), pp. 1365-66.
9. B. Lustman and F. Kerze, Jr.: *The Metallurgy of Zirconium, National Nuclear Energy Series*, McGraw Hill, New York, NY, 1965, p. 491.
10. I. Aitchison and B. Coxi: "Interpretation of Fractographs of SCC in Hexagonal Metals," *Corrosion*, 1972, *28*, pp. 83-87.
11. R.J.H. Wanhill: "A Fractograph Analysis of Environmental Fatigue Crack Propagation in Ti-6Al-4V Sheet," *Corrosion*, 1976, *32*, pp. 163-72.
12. D.A. Meyn and E.J. Brooks: "Fractography and Material Science," *Special Technical Publication,* 733, L.N. Gilbertson and R.D. Zipp, ed., American Society for Testing and Materials, Philadelphia, PA, 1981, p. 5.